

# Optimization of Stack Emission Parameters Using Gaussian Plume Model

Zairi Ali, Ubaidullah, M. N. Zahid<sup>a</sup>, Kahar Osman\*

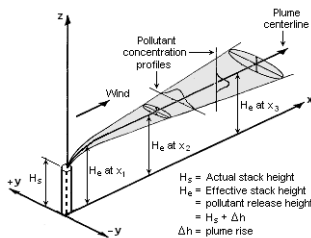
<sup>a</sup>Faculty of Mechanical Engineering, Universiti Teknologi Malaysia, 81310 UTM Johor Bahru, Johor, Malaysia

\*Corresponding author: kahar@fkm.utm.my

## Article history

Received :15 June 2012  
Received in revised form :12 August 2012  
Accepted :28 August 2012

## Graphical abstract



## Abstract

Numerical simulation is an economical way to control air pollution because of its consistency and ease of use compared to traditional data sampling method. The objective of this research is to develop a practical numerical algorithm to predict the dispersion of pollutant particles around a specific source of emission. The algorithm is tested with a rubber wood manufacturing plant. Gaussian-plume model were used as air dispersion model due to its simplicity and generic application. Results of this study show the concentrations of the pollutant particles on ground level reached approximately  $90\mu\text{g}/\text{m}^3$ , compared with other software. This value surpasses the limit of  $50\mu\text{g}/\text{m}^3$  stipulated by the National Ambient Air Quality Standard (NAAQS) and Recommended Malaysian Guidelines (RMG) set by Environment Department of Malaysia. The manufacturing plant is advised to make a few changes with its emission parameters and adequate values are suggested. In general, the developed algorithm is proven to be able to predict particles distribution around emitted source with acceptable accuracy.

**Keywords:** Numerical, dispersion, pollutant particles, Gaussian plume model

© 2012 Penerbit UTM Press. All rights reserved.

## 1.0 INTRODUCTION

Air pollution control is done by estimating the level of pollutant particles in the atmosphere by getting the concentration of the harmful particles in the atmosphere. The expensive cost of the measurement instruments and maintaining the measurement activities to get the data for ground-level concentration distribution are two of the major problems. Numerical prediction by air dispersion modeling is used as an alternative for air pollution control.

Air pollution controls textbook by Sutton (1953). Rapid developments in the 1950's and 1960's, including major field studies and advances in the understanding of the structure of the atmosphere, led to the development of the first regulatory air pollution models in the U.S. The textbooks by Pasquill (1974) and Stern (1976) review much of the research and theory up until the mid 1970's. However, the proliferation of air pollution research and models to date has made it necessary to read specialized journals and conference proceedings to keep up with developments.

A dispersion model is essentially a computational procedure for predicting concentrations downwind of a pollutant source based on the emissions characteristics (stack exit velocity, plume temperature, stack diameter, etc.), terrain (surface roughness, local topography, nearby buildings) and state of the atmosphere (wind speed, stability, mixing heights, etc.). The model should be able to predict rates of diffusion based on measurable meteorological variables such as wind speed, atmospheric turbulence and thermodynamic effects.

The air dispersion models consist of Box model, Gaussian model, Lagrangian model, Eulerian model and Dense gas model. Box model is very limited in its ability to accurately predict dispersion of air pollutants over an airshed because the assumption of homogeneous pollutant distribution is much too simple. Gaussian model assumes that the air pollutant dispersion has a Gaussian distribution, meaning that the pollutant distribution has a normal probability distribution. Gaussian models are most often used for predicting the dispersion of continuous, buoyant air pollution plumes originating from ground-level or elevated sources (Beychok, 2005). Gaussian models may also be used for predicting the dispersion of non-continuous air pollution plumes called puff models (Jung *et al.*, 2003). Lagrangian dispersion model mathematically follows pollution plume parcels (also called particles) as the parcels move in the atmosphere and they model the motion of the parcels as a random walk process. The Lagrangian model then calculates the air pollution dispersion by computing the statistics of the trajectories of a large number of the pollution plume parcels. A Lagrangian model uses a moving frame of reference as the parcels move from their initial location. A Eulerian dispersions model is similar to a Lagrangian model in that it also tracks the movement of a large number of pollution plume parcels as they move from their initial location. The most important difference between the two models is that the Eulerian model uses a fixed three-dimensional Cartesian grid as a frame of reference rather than a moving frame of reference. Dense gas models simulate the dispersion of dense gas plumes (i.e., pollution plumes that are heavier than air). The three most commonly used dense gas models are the DEGADIS model developed by Dr.

Jerry Havens and Dr. Tom Spicer at the University of Arkansas under commission by the US Coast Guard and the US Environmental Protection Agency. Second, the SLAB model developed by the Lawrence Livermore National Laboratory funded by the US Department of Energy, the US Air Force and the American Petroleum Institute. Lastly, the HEGADAS model developed by Shell Oil's research division. DEGADIS model uses empirical similarity profile for the concentration that expresses the model in terms of center-line ground level concentration meanwhile, HEGADAS model uses mathematical formulation originated by Colenbrander (1984) for both steady-state and transient release (Wilttox, 1994).

Researches on Gaussian plume model in the past decades are prone to developing the model with additional formulas and parameters to generalise the application of the model. The improvement of the model has been done by many researchers such as study on the effect of elevated release for the model (Robertson and Barry, 1988) and integrate emission source and meteorological data and display (maps of pollution levels) with the Gaussian plume model for instantaneous emission in a single algorithm (Arystanbekova, 2004). Huber (1990) studied the effect of building downwash on the dispersion of Gaussian model. However, the study limits to very specific cases and provides a base in validating the Gaussian plume model with wind tunnel model used in the study. During the deposition of SO<sub>2</sub> and NO<sub>x</sub>, the formation of secondary pollutants of sulphate and nitrate aerosols and their effects on the ground concentration of Gaussian plume model also has been studied (Tsuang, 2003). Carlson and Arndt (2007) developed the specific Gaussian plume model for Oklahoma area. The model integrated current weather condition and future weather forecast to enable prediction of future atmospheric dispersion.

Apart from the ability to predict the ground concentration of emission source, Gaussian plume model is also applied to estimate the source emission rate by using an inverse algorithm of the model. Lushi (2009) developed a method based on Ermak's Gaussian plume type solution to the advection-diffusion for estimating contaminant emissions using linear least square approach.

A few case studies proved that applying Gaussian plume model to selected harmful particle sources in industries still possess important role in pollution research. Leroy *et al.* (2010) evaluates the level of safety at a nuclear fuel reprocessing plant at ARENA NC facility in France by predicting the distribution of krypton-85 around the plant. Sadeghi and Sadrnia (2011) studied the cancer risk assessment by simulating the dispersion of radionuclide from Tehran research reactor using Gaussian plume computer code (CAP88-PC). Meanwhile, present study selected a rubber wood manufacturing plant to apply the Gaussian model algorithm developed in this research.

For long range transport, Gaussian plume model suffers from over estimate the particle concentrations for distances 10 km and above. The comparison between Gaussian plume model, PLUME and langrangian model, NAME has been done by Lutman *et al.* (2003) and found that Gaussian model is still applicable for long range transport of pollutants but NAME is more realistic in visual results. Both PLUME and NAME have small variation of ground-level concentration values.

The amount of turbulence can be categorized into define increments or stability classes. Pasquill stability classes categorized the amount of turbulent by A, B, C, D and E classes. Class A denotes the most unstable or most turbulent condition, and class F denotes the most stable or least turbulent condition. Appendix A – Table 2.1 lists the six classes (European Process Safety Centre, 1999). Atmospheric air turbulence is created by many factors, such as: wind flow over rough terrain, trees or

buildings, migrating high and low pressure air masses and fronts which cause winds, thermal turbulence from rising warm air, etc.

## 2.0 AIR DISPERSION MODELING

The Gaussian plume model was used as air dispersion model due to its simplicity and generic applications. The methodology and most of the formulas and parameters were obtained from Beychok (1979). The hourly concentration at downwind distance  $x$  (meters), crosswind distance  $y$  (meters) and receptor height ( $Z_r$ ) is given by general equation.

$$C_{x,y,z_r} = \frac{Q}{2\pi u \sigma_y \sigma_z} \exp\left[-\frac{1}{2}\left(\frac{y}{\sigma_y}\right)^2\right] \left\{ \exp\left[-\frac{1}{2}\left(\frac{z_r - h_e}{\sigma_z}\right)^2\right] + \exp\left[-\frac{1}{2}\left(\frac{z_r + h_e}{\sigma_z}\right)^2\right] \right\} \quad (1)$$

Eq. (1) is valid within these summarized constraints (Beychok, 1979) and can be visualised using Figure 1:

- i. Vertical and crosswind diffusion occur according to Gaussian distribution.
- ii. Downwind diffusion is negligible compared to downwind transport by the wind.
- iii. The emissions rate,  $Q$ , is continuous and constant.
- iv. The horizontal wind velocity and the mean direction are constant.
- v. There is no deposition, washout, chemical conversion or absorption of emissions, and any emissions diffusing to the ground are reflected back into the plume (all emissions are totally conserved within the plume).
- vi. In general, the effects on ambient concentrations of gravitational settling and dry deposition can be neglected for gaseous pollutants and small particulates (less than about 0.1 microns in diameter).
- vii. There is no upper barrier to vertical diffusion and there is no crosswind diffusion barrier
- viii. Emissions reflected upward from the ground are distributed vertically as if released from an imaginary plume beneath the ground and are additive to the actual plume distribution.
- ix. The use of  $u$  and  $\theta$  as constants at a given downwind distance, and the assumption of an expanding conical plume, implicitly require homogeneous turbulence throughout the  $x$ ,  $y$  and  $z$  dimensions of the plume.

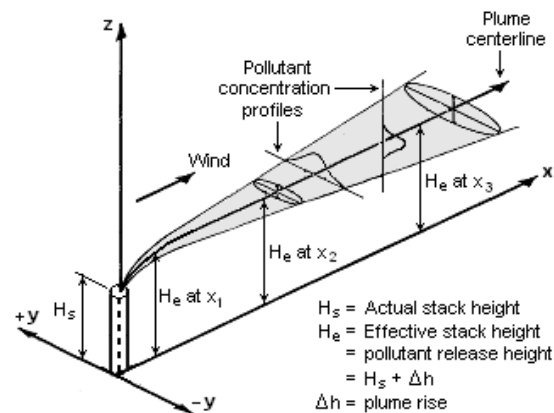


Figure 1 Atmospheric dispersion plume with Gaussian distribution (Beychok, 2005)

For prediction in rural area, the equations developed by U.S. EPA, 1995 that approximately fit the Pasquill-Gifford curves (Turner, 1970) has been used and for urban area, equations were determined by Briggs and represent the best fit to urban vertical diffusion data reported by McElroy and Pooler (1968).

The Gaussian-plume formula is derived by assuming steady-state conditions. Thus, the Gaussian-plume dispersion formulae do not depend on time. The meteorological conditions are assumed to remain constant during the dispersion from source to receptor, which is effectively instantaneous. The algorithm developed in the present study able to predict the hotspot region which has ground level concentration higher than the allowable value stipulated by National Ambient Air Quality Standard (NAAQS) and Recommended Malaysian Guidelines (RMG).

**3.0 RESULTS AND DISCUSSION**

The algorithm of Gaussian Plume Model developed for results in present study were compared between Schnelle and Dey (2000) and Industrial Source Complex-PC (ISCPC) software. The stability classes ranged from A (very unstable) to F (stable) in which unstable classes represent high turbulence atmosphere while stable classes are the opposite. Formaldehyde and dim-Ether properties were used. The Briggs equations were used to represent the plume rise.

Figure 2 shows the concentration isopleths as a result of output display for present study. With the same input data, Concentration Isopleths and Plume Centerline Concentration graph are acquired as indicated in Figure 3 for a comparison with Schnelle and Dey. The results had a small variaton of 0.46 km (7.67 %) for maximum ground-level concentration. However, this difference doesn't mean Schnelle and Dey have more accurate predictive results over present study. The methodology that had been used by Schnelle and Dey may be different from the methodology used in present study. However, methodology, formulas, and parameters which are being used here are more up-to-date.

Area mode: Rural

**Table 1** Inputs Data of Schnelle and Dey [5] (a)

Input Data	Stack height (m)	Stack diameter (m)	Stack temperature (K)	Exit velocity (m/s)	Stack gas volumetric flow rate (m <sup>3</sup> /s)
Stack	91.50	3.05	394	13.70	375.30

(b)

Input Data	Ambient Temperature (K)	Stability class	Wind speed (m/s)	Anemometer height (m)	Mixing height (m)
Atmospheric	294	D	5	91.50	0.00

**Table 2** Comparison Result with Schnelle and Dey [5]

Result	Schnelle and Dey	Present Study
Max Concentration, µg/m <sup>3</sup>	110	109.9604
Downwind Distance, km	6	5.5400

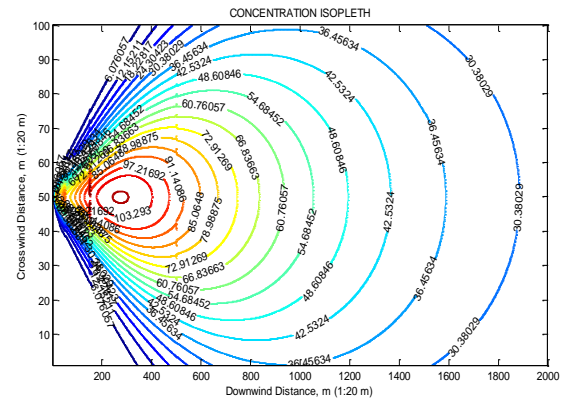


**Figure 2** Concentration Isopleth (µg/m<sup>3</sup>) from present study

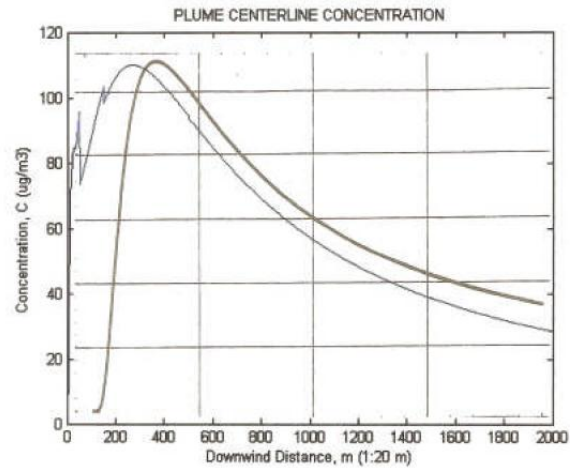


**Figure 3** Comparison with Schnelle and Dey [5]

The input data used are shows in Table 3. With the same input data, from Plume Centerline Concentration graph in Figure 4, the maximum ground-level concentration is 86.9621 µg/m<sup>3</sup> at downwind distance of 0.7 km compared with ISCPC that gives maximum ground-level concentration 92.4390 µg/m<sup>3</sup> at the downwind distance of 1.16 km from the source. This comparison value indicated in Table 4. Concentration Isopleths graph as shown on Figure 4 is the result from the present study. The difference between the values of present study and ISCPC software for maximum concentration is 5.4769 µg/m<sup>3</sup> (4.97 %) and 0.46 km (7.67 %) for downwind distance. ISCPC software uses U.S. EPA ISC algorithm and present study uses standard Gaussian plume model equation to obtain results.

Area mode: Rural

**Table 3** Inputs Data of ISCPC Software and Present Study (a)

Input Data	Stack height (m)	Stack diameter (m)	Stack temperature (K)	Exit velocity (m/s)	Stack gas volumetric flow rate (m <sup>3</sup> /s)
Stack	68.58	2.096	394.3	12.2	47.25

(b)

Input Data	Ambient Temperature (K)	Stability class	Wind speed (m/s)	Anemometer height (m)	Mixing height (m)
Atmospheric	291.48	B	2.5	10.0	3000

**Table 4** Comparison Result with ISCPC Software

Result	ISCPC Software	Present Study
Max Concentration, $\mu\text{g}/\text{m}^3$	92.4390	86.9621
Downwind Distance, km	1.16	0.7

**PLUME CENTERLINE CONCENTRATION**

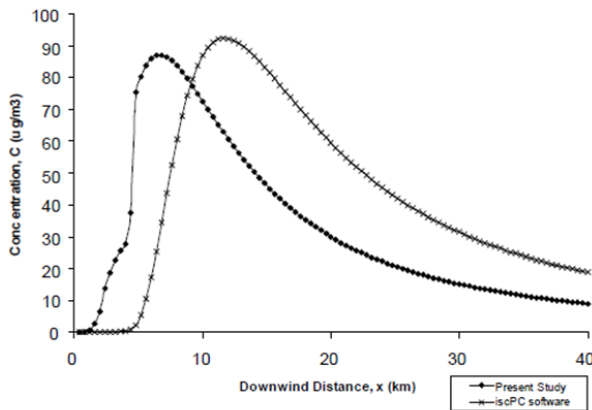


**Figure 4** Comparison with ISCPC Software

The preceding comparisons are sufficient to ensure that the results obtained from the algorithm in the present study is relevant to simulate the dispersion of pollutant particles. The results as in Figure 5, Figure 6, Figure 7, Figure 8, Figure 9, shows the effect of emission variables on the concentration distribution of pollutant particles in downwind direction. We can predict the hot spot region of the simulated particle dispersion by taking the downwind distances with pollutant concentration higher than the allowed value by RMG and NAAQS. For this case, the ground level concentration must not exceed  $50\mu\text{g}/\text{m}^3$ . As for example, the graph of velocity increase in Figure 5 has a hot spot region for stack exit velocity lower than 32m/s. For exit velocity of 32m/s, it has approximately 0.1 km in diameter of area with ground level concentration higher than  $50\mu\text{g}/\text{m}^3$  and the area increases as the exit velocity decreases. This area also increases as the maximum concentration value increases.

A study on Evergreen Fibreboard has been conducted to consult the company to control their stack emission variables. The data provided by AMR Environment Sdn Bhd includes Formaldehyde and dim-Ether but only results of dim-Ether are shown in this paper. Table 5 shows input data for dim-Ether.

**Table 5** Input Data of Present Study for Evergreen Fibreboard

Input Data	Stack height (m)	Stack diameter (m)	Stack temperature (K)	Exit velocity (m/s)	Stack gas volumetric flow rate (g/s)
Stack	38	0.4572	308	17.8	2.94789

(b)

Input Data	Ambient Temperature (K)	Stability class	Wind speed (m/s)	Anemometer height (m)	Mixing height (m)
Atmospheric	299.7	A	0.8	10.0	256

Figure 5 shows Plume Centerline Concentration by increasing the exit velocity in increments of 20% till the exit velocity is 200% increase from the baseline value. It is proved that increasing stack exit velocity has impact on lowering the maximum ground-level concentration. One of the simple ways to increase the velocity is by using a larger power fan. However, increasing velocity about 100% to 35.60 m/s is already enough to reduce maximum concentration to  $44.6834\mu\text{g}/\text{m}^3$  and follow the limit in RMG and NAAQS. However, the effective range of velocity increase to reduce maximum concentration is about 20% to 160%. This is because the percent change of maximum concentration will become constant (percent difference about 4%) for increasing velocity above 160%. For 20% stack exit velocity increase and below, it has no effect on the location that has maximum ground-level concentration. However for higher velocity increase the location changed. The location for maximum ground-level concentration changes from 240m to 270m in the downwind distance for 70% stack exit velocity increase. It also changing from 270m to 300m for 200% stack exit velocity increase. It is important to monitor the distance so that maximum concentration will not occur at residential area.

**PLUME CENTERLINE CONCENTRATION**

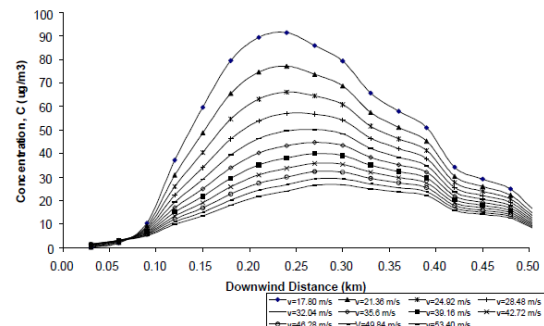


**Figure 5** Effect of velocity increase

For stack height, stack exit temperature and stack diameter as in Figure 6, Figure 7 and Figure 8, Increasing the stack height about 60% to 60.8 m, Increasing the stack exit temperature about 40% to 431.2 K and reducing 0.2514 m for diameter are already enough to reduce maximum concentration to  $50\mu\text{g}/\text{m}^3$  and follow the limit in RMG and NAAQS. The effective range of increasing stack height to reduce maximum concentration is about 20% to 120% (percent difference about 2% for 120% and above).



Downwind distance which is maximum ground-level concentration occurs, changed from 240 m to 270 m when stack height is increased up to 20% and which is more sensitive than changing exit velocity. Smaller range of increasing stack height compared with increasing exit velocity proved that changing stack height has larger effect in reducing the maximum concentration. For the second case of decreasing stack diameter, exit velocity is kept constant which reduces emission flow rate, result from Figure 9 shows that the Plume Centerline Concentration increases with decreasing stack diameter for this case. For changing the baseline input data (rural to urban), the maximum concentration has increase about 64.16% from 91.3991  $\mu\text{g}/\text{m}^3$  to 150.0385  $\mu\text{g}/\text{m}^3$ .

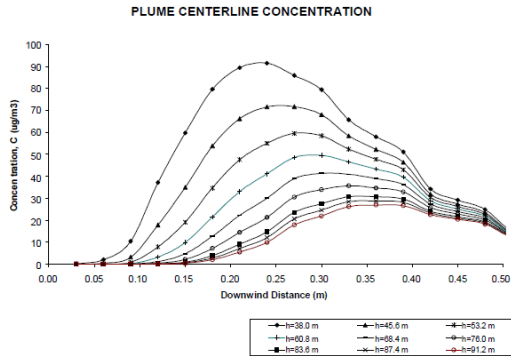


Figure 6 Effect of stack height increase

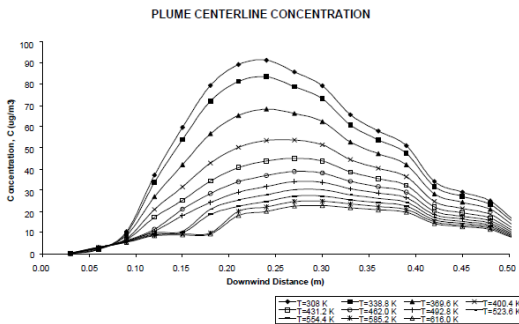


Figure 7 Effect of stack exit temperature increase

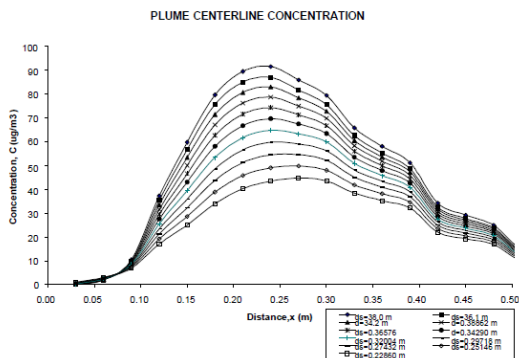


Figure 8 Effect of stack diameter decrease (changing stack exit velocity, keeping constant exit flow rate)

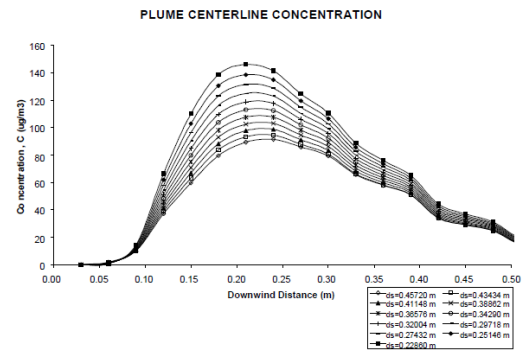


Figure 9 Effect of stack diameter decrease (no change in stack exit velocity)

Based on Figure 10, urban area causes higher maximum ground concentration. It increases by approximately 65% from 91.3991  $\mu\text{g}/\text{m}^3$  to 150.0386  $\mu\text{g}/\text{m}^3$ . In Figure 12, the changing rate of pollutant concentration with different stability classes is shown. Stability class A tends to have the highest value of maximum concentration compared to other classes. It is important to consider the A stability class as it produces more than 100% ground level concentration than the others. During the simulation, we should consider all stability classes before declaring the preprocessing input data are allowed to be practiced. However, for factories located in the area with ambient wind speed faster than 2.5 m/s (stability classes B to F), the emission is less restricted as in Table 6. That is because faster ambient wind speed disperse the pollutant particles in a longer distance than slower wind speed. It will cause the pollutants to distribute better along the downwind distance with lower value of ground level concentration.

Table 6 Effect of atmospheric condition to maximum concentration

Stability	Wind Speed (m/s)	Concentration ( $\mu\text{g}/\text{m}^3$ )	Distance (m)	Concentration Decrease (%)
A	0.8	91.3991	240	0.00
B	2.5	34.5995	300	62.14
C	2.5	33.8523	480	62.96
D	4.0	18.2806	900	80.00
E	5.0	5.2458	1650	94.26
F	5.0	3.8211	1980	95.82

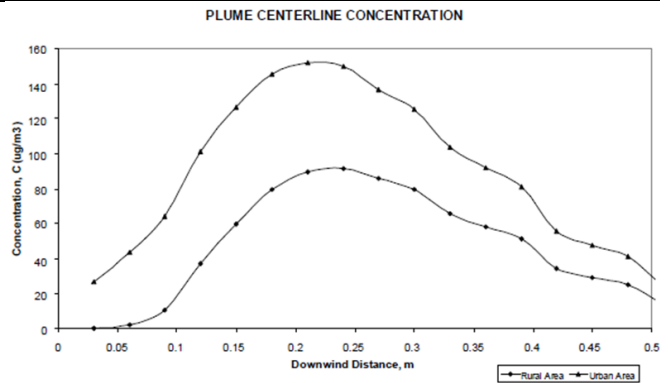


Figure 10 Plume Centerline Concentration for rural and urban mode

The effects of atmospheric condition are shown in Figure 11 and Figure 12. Stability condition ranged from A to F and all other parameters, except wind speed (which often changes with

stability condition) are constant. It should be noted that the stability conditions depend on whether it is daytime or nighttime, the degree of insolation (incoming solar radiation), and the cloudiness and other factors. Even though Stability A has calmer wind speed, the concentration are still higher than the others. For the same wind speed, under different atmospheric condition (stability), unstable conditions have higher concentration (In this case, stability class B & C, E & F). As atmospheric condition become more stable (goes from A to F), the effect on maximum ground-level concentration goes down significantly. At the same time, the maximum ground-level concentration tends to occur at larger distances from the emitted source, implying that at a certain distance from the source, the ground-level concentration may be higher under unstable condition than stable conditions.

Figure 13 shows the effect of reducing mass flowrate of dim-Ether to the concentration distribution along the downwind distance. It can be seen that the factory emits more dim-Ether than the allowable amount suggested by RMG and NAAQS. The maximum concentration occurs at approximately 200m away from the factory stack. The Figure shows that by reducing the flowrate from 2.94789 g/s to 0.96597 g/s (about 60%) is enough to reduce the maximum ground level concentration to the allowable value. In case that the factory are not permitted to emit lower than a certain value of mass flowrate, two or more emission variables need to be optimized simultaneously. For example, if 70% (2.06352g/s) of current mass flowrate is the minimum limitation, then stack exit velocity can be increased from 17.8m/s to 31.5 m/s in order to follow the regulation. However, the discussed value is for stability class A which rarely occurred in most atmospheric condition. Other stability classes tends to have lower value of concentration and much safer in practice but stability class A is used as the simulation benchmark.

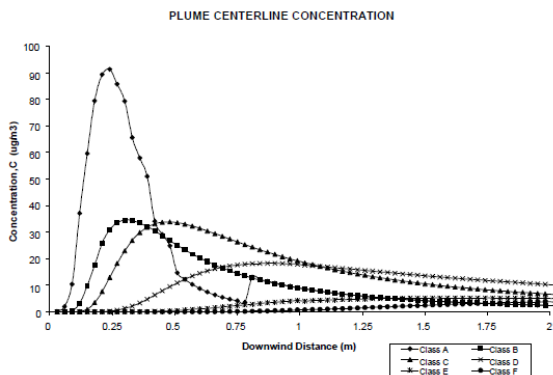


Figure 11 Plume centerline concentration for different stability

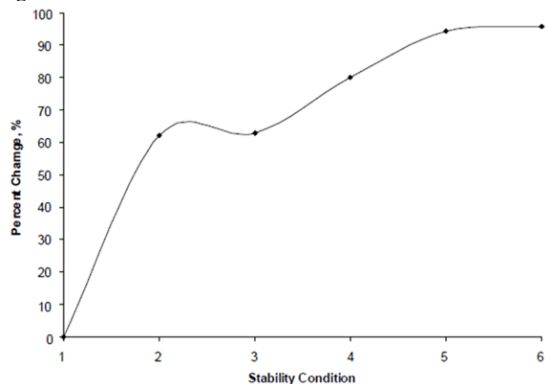


Figure 12 Plume Centerline Concentration for different stability

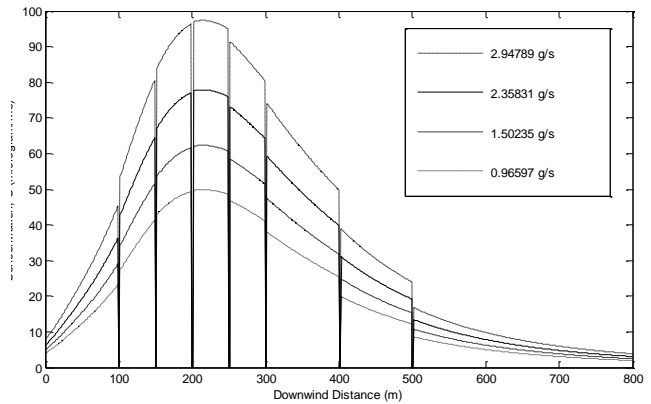


Figure 13 Plume centerline concentration for different mass flowrate

### Acknowledgement

The author, Ubaidullah would like to thank the academic staff of the Universiti Teknologi Malaysia for their great help and sincere assistance in dealing with the studied subject throughout the period of this work. The author also would like to acknowledge the Universiti Teknologi Malaysia for the support of this research.

### Nomenclature

$Q$	Pollutant emission rate, g/s
$u_s$	Wind speed adjusted to release height, m/s
$x$	Downwind distance from source to receptor, m
$y$	Crosswind distance from source to receptor, m
$z$	Receptor/terrain height above mean sea level, m
$z_r$	Receptor height above ground level, m

### References

- [1] O. G. Sutton. 1953. *Micrometeorology*. London: McGraw-Hill.
- [2] F. Pasquill. 1974. *Atmospheric Diffusion*. 2<sup>nd</sup> edition. Chichester: Ellis Horwood Limited.
- [3] A. C. Stern. 1976. *Air Pollutants, Their Transformation and Transport*. New York: Academic Press.
- [4] M. R. Beychok. 1979. *Fundamentals Of Stack Gas Dispersion*. Irvine, California.
- [5] K. B. Schnelle and P. R. Dey. 2000. *Atmospheric Dispersion Modeling Compliance Guide*. United State of America: McGraw-Hill.
- [6] N. K. Arystanbekova, *Application of Gaussian Plume Models for Air Pollution Simulation at Instantaneous Emissions*. 2004. Mathematics and Computer in Simulation.
- [7] H. W. M. Witlox. 1994. *The HEGADAS Model for Ground-Level Heavy-Gas Dispersion – I. Steady-State Model*. Atmospheric Environment. 28: 2917–2932.
- [8] A. H. Huber. 1991. *Wind Tunnel and Gaussian Plume Modeling of Building Wake Dispersion*. Atmospheric Environment. 25(A): 1237–1249.
- [9] E. R. Lutman et al. 2004. Comparison Between the Predictions of a Gaussian Plume Model and a Lagrangian Particle Dispersion Model for Annual Average Calculations of Long-Range Dispersion of Radionuclides. *Journal of Environmental Radioactivity*. 339–355.

- [10] E. Robertson and P. J. Barry. 1998. *The Validity of A Gaussian Plume Model When Applied to Elevated Releases at A Site On The Canadian Shield*. Atmospheric Environment. 21: 351–362.
- [11] E. Lushi, J. M. Stockie. 2009. An Inverse Gaussian Plume Approach for Estimating Atmospheric Pollutant Emissions from Multiple Point Sources. *Atmospheric Environment*. 44: 1097–1107.
- [12] C. Leroy, D. Maro, D. Hebert, L. Solier, M. Rozet, S. Le Cavelier, O. Connan. *A Study of the Atmospheric Dispersion of a High Release of Krypton-85 above a Complex Terrain, Comparison with the Predictions of Gaussian Models*. 2010. Journal of Environmental Radioactivity. Vol 101, pp: 937-944.
- [13] B. J. Tsuang. *Quantification on the source/receptor relationship of primary pollutants and secondary aerosols by a Gaussian plume model*. 2003. Atmospheric Environment. Vol 37, pp:3981-3991.
- [14] J. D. Carlson and D. S. Arndt. *The Oklahoma Dispersion Model : Using Gaussian Plume Model as an Operational Management Tool for Determinaing Near- Surface Dispersion Conditions across Oklahoma*. 2006. Journal of Applied Meteorology and Climatology. Vol 47.
- [15] N. Sadeghi and M. Sadrnia. *Cancer risk assessment for Tehran research reactor and radioisotope laboratory with CAP88-PC code (Gaussian plume model)*. 2011. Nuclear Engineering and Design. Vol 241, pp:1795-1798.
- [16] M. R. Beychok. 2005. *Fundamentals of Stack Gas Dispersion*. 4<sup>th</sup>Edition. Irvine, California.
- [17] Y. R. Jung, W. G. Park, O. H. Park. *Pollution Dispersion Analysis using the Puff Model with Numerical Flow Field Data*. 2003. Mechanics Research Communication. 30: 277–286.